

## Parametric analysis on hybrid design method for steel cellular beams

<http://dx.doi.org/10.1590/0370-44672023770076>

Lucas Alves de Aguiar<sup>1,2</sup>

<https://orcid.org/0009-0002-7542-6201>

Matheus Erpen Benincá<sup>1,3</sup>

<https://orcid.org/0000-0003-4852-6127>

Inácio Benvegno Morsch<sup>1,4</sup>

<https://orcid.org/0000-0002-2473-3474>

<sup>1</sup>Universidade Federal do Rio Grande do Sul – UFRGS, Departamento de Engenharia Civil, Programa de Pós-Graduação em Engenharia Civil, Porto Alegre - Rio Grande do Sul - Brasil.

E-mails : <sup>2</sup>[lucas.a.aguiar@hotmail.com](mailto:lucas.a.aguiar@hotmail.com),

<sup>3</sup>[matheuseb@hotmail.com](mailto:matheuseb@hotmail.com), <sup>4</sup>[morsch@ufrgs.br](mailto:morsch@ufrgs.br)

### Abstract

Cellular beams are an attractive engineering solution due to their high strength to weight ratio, allowing for a design even lighter and more cost efficient in steel structures. These beams possess enhanced strength and stiffness compared to regular I-section beams of similar weight, due to their higher second moment of area. However, their variable cross-sections along the length introduce different modes of failure, making further research necessary, since there is a lack of standardized processes for their design. This paper investigates the design and verification procedures proposed by Ward (1990), Annex N (1998), Veríssimo *et al.* (2013), Fares *et al.* (2016), and Grilo *et al.* (2018) through a parametric study of cellular beams with varying geometries. To assess the buckling characteristics of cellular beams, shell finite element models are employed, which were previously validated, using experimental tests conducted by other researchers. The results obtained from a Python code implementing these design methods are then compared with Finite Element Method (FEM) analysis results for 80 beams. It can be concluded that the design methods provide conservative results for beams with intermediate or long spans. On the other hand, for beams with short spans, these methods may yield values that compromise safety. Finally, based on the FEM analysis results, a Hybrid Design Method (HDM) is proposed, which incorporates the verification procedures analyzed. This proposed method presents a better failure mode detection and limited load capacity when applied to cellular beams made from regular Brazilian I-section beams.

**Keywords:** cellular beams; parametric analysis; finite elements method; failure modes; design method.

### 1. Introduction

A cellular beam is a type of alveolar beam that is manufactured through three main steps: (1) make double longitudinal cuts in the web of regular I-section beams; (2) separate two web parts and relocate to form circular openings; and (3) weld the two parts of the beam together. The geometry of the cellular beams provides advantages in the bending stiffness and strength-to-weight ratio compared to regular I-section beams. Also, these beams are suitable for office buildings, parking garages, shopping centers, and any structure with a suspended floor. On the other hand, the web openings can reduce the shear strength capacity. Cimadevila *et al.* (2000) explain that these beams work with relatively low stresses, and the best use of the material

is conditioned to the optimization of the second moment of area of the section, aiming to minimize deflections.

Several physical phenomena related to Ultimate Limit States (ULS) must be considered to assess the structural behavior of steel cellular beams, such as local and global buckling and plastic hinge formation. Kerdal and Nethercot (1984) first evaluated the behavior of castellated beams, alveolar beams with hexagonal openings, which identified six potential failure modes: Formation of the Vierendeel Mechanism (FVM), Web-Post Buckling (WPB), Rupture of Welded Joints (RWJ), Lateral-Torsional Buckling (LTB) of an entire span, and Formation of a simple Flexure Mechanism (FFM), where plastic yielding occurs in pure bending of the tee section above or below the beam. These

failure modes depend on the special geometry of these beams, web slenderness, geometry of openings, types of loading, and lateral support provision.

The geometry of cellular beams depends on the beam manufacturing process. In this regard, the double-cut method allows for more flexible configuration of openings than in castellated beams. Even so, the six failure modes determined by Kerdal and Nethercot (1984) can also be found in cellular beams. Firstly, under the supervision of the Steel Construction Institute (SCI), full-scale destructive tests were conducted at Bradford University to confirm the structural integrity and design criteria of cellular beams (Lawson, 1988). Later, Ward (1990) incorporated the experimental results to investigate the buckling behavior of the web-post

through a series of nonlinear Finite Element Method (FEM) analysis. In addition to the numerical data, analytical studies were conducted and a design method for cellular beams was proposed.

After that, some researchers investigated specific failure modes. Chung *et al.* (2001) presented a comprehensive analysis of the Vierendeel mechanism in steel cellular beams. The authors described the behavior of these beams and derived their flexural, local, web-post strengths, as well as the bending modes of both non-composite and composite cellular beams through a detailed parametric study using FEM analysis. Warren (2001) tested eight full-scale cellular beams that failed by the Vierendeel mechanism. A nonlinear finite element analysis complemented his study, and the author compared the results using the methodology proposed by Ward (1990). While these studies provide valuable insights into the FVM failure, it is imperative to assess them in conjunction with evaluations of other potential failure modes, since in the design of cellular beams other failure modes may occur before the Vierendeel mechanism. Adopting an integrated approach to failure analysis becomes essential to evaluate the structural integrity and safety of these structural elements.

With a parametric analysis using a numerical model, Panedpojaman *et al.* (2014) provide a simplified method to estimate a horizontal shear strength for cellular beams for Web Post Buckling (WPB), considering a geometric factor and offering improved design equations for safe and cost-effective design. The model they used was an evolution of the one developed by Lawson and Hicks (2011) based on a strut model. After that, Grilo *et al.* (2018) developed a numerical model in ABAQUS and validated it through an experimental testing program. The authors considered a perfect elasto-plastic behavior for steel in this finite element model and represented the beam using shell elements. Then, a buckling formulation of web capacity

## 2. Design Methods

When designing a cellular beam, it is crucial to verify both its strength (ULS) and serviceability (SLS). Therefore, various constraints need to be considered, such as displacement limitations, overall beam flexural capacity to verify a FVM failure, beam shear capacity to verify an RWJ failure, and LTB checks,

was proposed based on the parametric analysis. The experimental tests made by Grilo *et al.* (2018), and complemented by the Tsavdaridis and D'Mello (2011) experiment, served as validation of the numerical model developed in ABAQUS proposed by Shamass and Guarracino (2020). This model considered an elasto-plastic material and uses von Mises yield criterion with associated plastic flow and isotropic hardening. Based on parametric analyses using this numerical model, a verification formulation for WPB failure was developed based on the shear model by Ritter and Morsch. These studies evaluate and propose equations to analyze a WPB failure. However, it is important that they are evaluated in a context combined with a cellular beam design method involving all failure modes.

Sonck and Belis (2015) conducted a parametric analysis of web openings in steel beams to investigate failure caused by LTB. They developed a finite element model in ABAQUS software and validated it with experimental tests at Ghent University (Sonck, 2014). The strength of each opening was determined using a Newton-Raphson analysis with the Arc-length technique. The analysis accounted for geometric imperfections and employed an elasto-plastic model. The authors proposed a simplified method for verifying failure due to torsional lateral buckling based on their study. This study only evaluates one failure mode, in beams that are not laterally braced. However, for optimal cellular beam design, it is necessary to evaluate the request by checking all possible failure modes.

More recently, Braga *et al.* (2021) developed a design approach to evaluate the beam's load capacity with standard geometries inspired by the Direct Strength Method. Their parametric study found that beam length affects bending failure modes, while the slenderness ratio influences the beam buckling. The proposed method aligned with finite element results, considering initial imperfections, inelastic

where these failures are similar to corresponding modes for solid web beams. However, WPB and Formation of the Vierendeel Mechanism (FVM) are failures that occur specifically in cellular beams. Furthermore, WPB can manifest in two distinct forms. The first occurs due to a compressive load on the web post, leading

material behavior, and post buckling effects. However, it is noteworthy that the study focused exclusively on castellated beams, limiting its applicability to beams with higher geometric variability, such as cellular beams. However, while this study thoroughly evaluates all failure modes and compares with the Guide 31 design method by Fares *et al.* (2016), it primarily focuses on the analysis of castellated beams, which have a more restrictive geometry compared to cellular beams. As emphasized by Erdal and Saka (2023), there are limitations in both experimental and theoretical research on cellular beams when compared to castellated beams. Therefore, it is important to carry out a study that evaluates already consolidated cellular beam design methods.

As there is no specific technical standard for the design of cellular beams in Brazil and given the absence of a comprehensive comparison among international methods for cellular beam design and with FEM analyses, the importance of conducting the present study is justified. Therefore, this paper aims to fill this gap and provides valuable analytic data on the behavior of cellular beams through numerical simulations performed with the design methods proposed by Ward (1990), Annex N (1998), Veríssimo *et al.* (2013), Fares *et al.* (2016), Grilo *et al.* (2018), using a Python code. For that purpose, a parametric analysis is performed with 80 different geometries of cellular beams. The results obtained from the design methods are compared with those obtained by finite element nonlinear analysis considering initial geometric imperfections. Finally, a combination of the failure mode verifications of the different design methods is proposed, creating a Hybrid Design Method (HDM), to better design cellular beams made from Brazilian regular I-section beams, with a better failure mode detection, and more accurate approximations of the ultimate load capacity, when compared to FEM analysis.

to a verification process is similar to the buckling of a simple post compression. The second form corresponds to double curvature buckling caused by horizontal shear forces acting at the midsection of the web post (Figure 1). Then, the compressive stresses that develop at one of the inclined edges of the opening lead to the WPB in

shear. The FVM occurs due to the development of four plastic hinges in the upper and lower sections above and below the

opening. This phenomenon arises from the combination of the global moment and the Vierendeel moment. The Vierendeel

moment, also referred to as secondary moment, results from the transfer of shear forces across the opening.

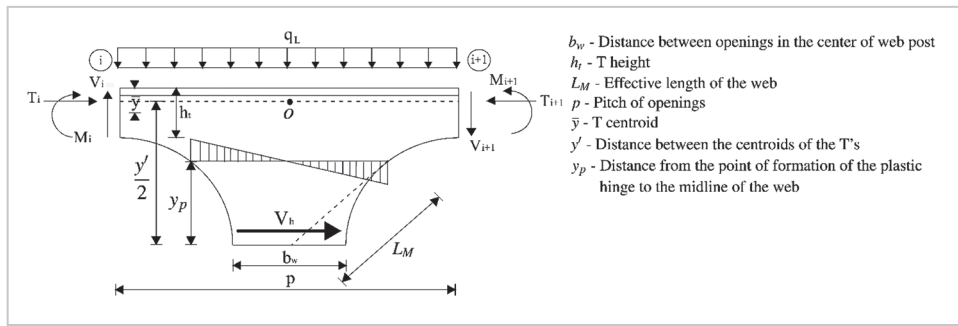


Figure 1 – Horizontal shear in the web-post of cellular beam.

In this study, five procedures are considered for the design and verification of cellular steel beams: (1) Veríssimo *et al.* (2013) (VER); (2) publication of Steel Construction Institute (SCI) by Ward (1990); (3) ASCI Design Guide 31 published by Fares *et al.* (2016) (GUIDE 31); (4) a design procedure of VER adopting the web buckling verification given by Grilo *et al.* (2018) (GRI); and (5) the Annex N (1998), which was an implementation proposal in the version of Eurocode ENV 1993-1-1:1992.

Then a Python code was developed in version 3.8.8, using Anaconda Spyder (2022) as an Integrated Development Environment (IDE) for open-source data analysis and scientific programming. The fundamental libraries used in this code were *numpy*, *scipy*, and *pandas*. This code, following the Object-Oriented Programming (POO) philosophy, serves the purpose of design cellular beams and consists of two modules: Design Procedures of Alveolar Beams (DPAB) and Numerical Analysis of Alveolar Beams (NAAB). The

first module is responsible for declaring a class in which attributes and methods are defined. The second module is responsible for creating objects (cellular beams) and, by incrementing the load in numerical analysis, utilizing the attributes and methods associated with that object. The latter is responsible for returning the attributes of the beam object in the current analysis, such as failure mode, failure load, and deflection obtained (Aguiar, 2023). The operating procedure of the Python code can be seen in Figure 2.

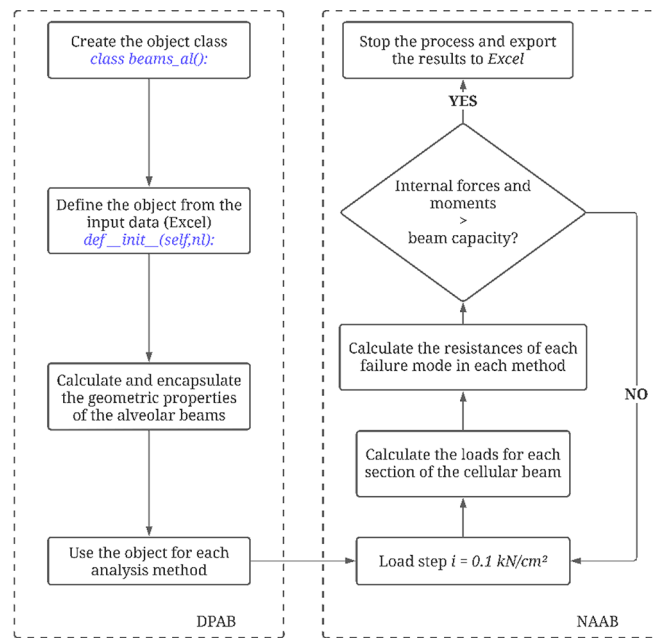


Figure 2 – Working process of the python code.

Although a structural engineer has the freedom to determine the circular opening diameter and spacing between their centers, it is essential to

follow the prescribed ratios in Equation 1, where Figure 3 shows the fundamental geometry and notations for these beams. It should be noted that the

Annex N - ENV (1998) design method is more restrictive, and the lower value ratio  $p / D_0$  is 1.25.

$$1.10 < \frac{p}{D_0} < 1.50 \text{ and } 1.25 < \frac{d_g}{D_0} < 1.75 \quad (1)$$

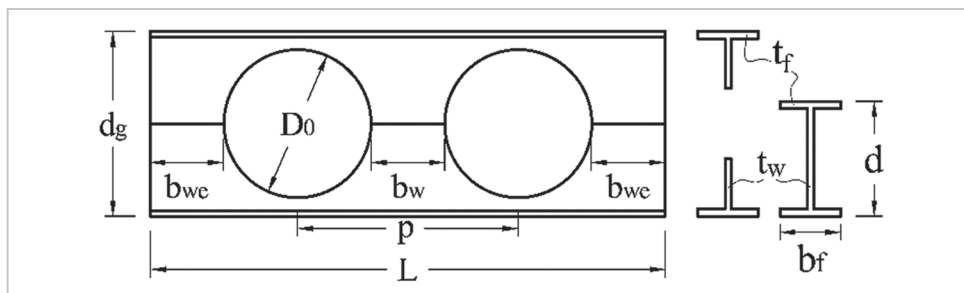


Figure 3 – Geometric parameters of a cellular beams.

### 3. Numerical Model

The behavior of the design methods is evaluated by numerical simulations with

the Finite Element (FE) model developed by Benincá and Morsch (2020), using ANSYS

APDL 2021R2. This section describes this numerical model and presents a validation study.

#### 3.1 Element and material modeling

The full-span beam was modeled using shell elements, with the 4-node element SHELL181, with 6 degrees of freedom per node, considering both membrane and bending stiffnesses. A

singular and centrally positioned layer was employed, featuring five integration points through the thickness. The beam was subdivided into smaller parts to create a mapped mesh network with

a maximum element size of 3 cm. A bilinear isotropic material model was used with the von Mises yield criterion, which effectively captures the nonlinear material behavior.

#### 3.2 Load application and boundary conditions

The model considered the cellular beam as simply supported, with the boundary conditions illustrated in Figure 4. Load application occurs in the nodes located in the upper flange,

allowing uniformly distributed or concentrated loads. In the latter case, the point of the concentrated load is specified. According to the beam geometry, the location of the stiffen-

ers in the web beam is determined by their position (x) and thickness. In addition, the location of the lateral supports is established to prevent a lateral (z-horizontal) displacement.

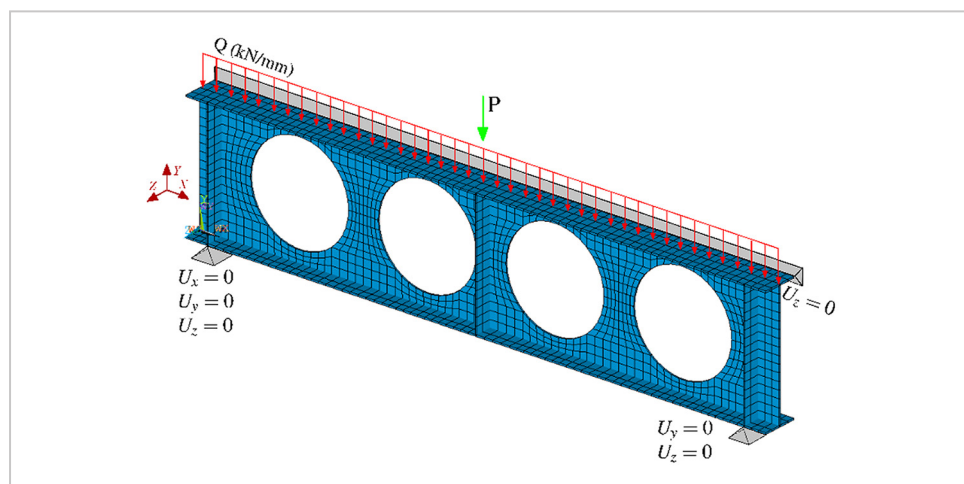


Figure 4 – Overview of a generic numerical model.

#### 3.3 Stages of solution

Four steps are performed to solve the numerical problem, defined as follows:

- A base static solution to define the geometric stiffness matrix;
- Elastic stability analysis to deter-

mine the instability modes and the associated critical loads;

- Addition of initial geometric imperfections to the beams, associated with some instability mode, in order to represent

irregularities on cellular beams;

- Nonlinear analysis, using the Newton-Raphson method associated with the Arc-Length technique, to determine the failure load, beam deflection, and failure mode.

#### 3.4 Initial geometric imperfection

Geometric imperfections aim to represent irregularities that may exist in the profile due to the manufacturing, storage, transportation, and assembly processes of the structure. In some studies with experimental results, such data may be

available, and in such cases, it can be considered for a numerical analysis aiming to replicate the experimental test. When practical data is not available, geometric imperfections need to be simulated. A well-established approach is to introduce

geometric imperfections through the instability modes of the beams. Therefore, Table 1 compiles studies that utilized instability modes as a means of incorporating geometric imperfections into their numerical models.

Table 1 - Geometric imperfections adopted in different studies.

Reference	Failure mode analyzed	Type of alveolar beam	Geometric Imperfection	Amplitude Factor
Soltani <i>et al.</i> (2012)	All failure mode	Castellated Beams	First buckling mode shape	$(d_g - 2t_f)/100$
Braga <i>et al.</i> (2021)	All failure mode	Castellated Beams	First buckling mode shape	$d_g/100$
Shamass and Guarracino (2020)	WPB	Cellular Beams	First buckling mode shape	$d_g/500$
Bake (2010)	WPB	Cellular Beams	First buckling mode shape	$d_g/600$
Panedpojaman <i>et al.</i> (2014)	WPB	Cellular Beams	First buckling mode shape	$d_g/500$
Grilo <i>et al.</i> (2018)	WPB	Cellular Beams	Double curvature mode shape	$d_g/3125$
Tsavdaridis and D'Mello (2011)	WPB	Cellular Beams	Double curvature mode shape	$t_w/200$
Sonck and Belis (2015)	LTB	Cellular Beams	Lateral-torsional buckling mode shape	$L/1000$

The studies by Grilo *et al.* (2018) and Tsavdaridis and D'Mello (2011) used a reduced model, whereupon both described that the mode used was double curvature. Sonck and Belis (2015) used the fault object of their study in a characteristic way: Lateral-Torsional Buckling. Therefore, in

this study, given the evaluation of a large number of beams and the lateral restraint of the top flange, meaning that lateral-torsional buckling (LTB) is not considered, the first mode shape of instability was adopted with an amplitude of  $d_g/600$ , as recommended by the study conducted by

Bake (2010). It is important to note that the combined selection of multiple instability modes for initial geometric imperfections can either increase or decrease the failure load of beams prone to buckling. Performing a detailed study for each case, which is not the focus of this work, is advisable.

### 3.5 Validation of FE modeling

The finite element model was developed and validated in the research of Benincá and Morsch (2020) and Benincá (2018), with several cellular and castellated beams analyzed, which were previously experimentally tested in other studies. Furthermore, to evaluate the main failure modes of cellular beams, three beams were selected and were experimentally tested by other authors, Warren (2001), Erdal and Saka (2013), and Grilo *et al.* (2018), with the aim of diversifying the validation of the numerical model. These specimens are named

2A, NPI240\_Test3, and A2, respectively, where the first one failed by the Vierendeel Mechanism, the second and third with WPB. The three specimens were simply supported and subjected to single concentrated loads at middle of span. The geometry of these beams is given in Table 2, and material properties of these beams is given in Table 3, where  $f_{yf}$  is the flange yield stress,  $f_{yw}$  is the web yield stress, and  $f_u$  is the ultimate steel stress of the beam.

Grilo *et al.* (2018) conducted experi-

mental measurements of geometric imperfections in Beam A2 and used the first instability mode, corresponding to the double curvature mode in the web, with an amplitude of  $d_g/4330$ . This value brought good results in the numerical analyzes by Grilo (2018). However, Erdal and Saka (2013) and Warren (2001) did not provide information on geometric imperfections for Beams NPI240\_test3 and 2A. Consequently, for these two beams, the approach recommended by Bake (2010) was adopted: employing the first instability mode with an amplitude of  $d_g/600$ .

Table 2 - Geometrical properties of three experiments cellular beams.

Reference	Specimen	$d$ mm	$t_w$ mm	$t_f$ mm	$b_f$ mm	$b_w$ mm	$d_g$ mm	$L$ mm	$D_0$ mm	$p/D_0$	$D_0/d$
Warren (2001)	2A	203	5.8	7.8	133.4	75	289.8	3800	225	1.33	1.11
Erdal and Saka (2013)	NPI-240 (test 3)	304.9	8.7	13.1	106	94	355.6	1423	251	1.27	1.13
Grilo <i>et al.</i> (2018)	A2	303	4.8	5.6	102	103.3	433	1874	342.5	1.3	1.14

Table 3 - Material properties of three experiments cellular beams.

Reference	Specimen	$f_{yw}$ MPa	$f_{yf}$ MPa	$f_u$ MPa	$E_w$ Gpa	$E_f$ Gpa
Warren (2001)	2A	347	320	430	187.89	196.74
Erdal and Saka (2013)	NPI-240 (test 3)	390	390	495	190	190
Grilo <i>et al.</i> (2018)	A2	416	416	480	188	188

Figure 5 presents a comparison between the FEM results, Experimental (Exp)

outcomes, and numerical results from the authors' finite element models (N.). The

numerical model demonstrates a favorable agreement with the experimental

load-displacement curves, effectively detecting the failure modes of the experi-

ments, with the failure modes obtained by the numerical simulation, being the

same as those observed in the experimental tests of these beams.

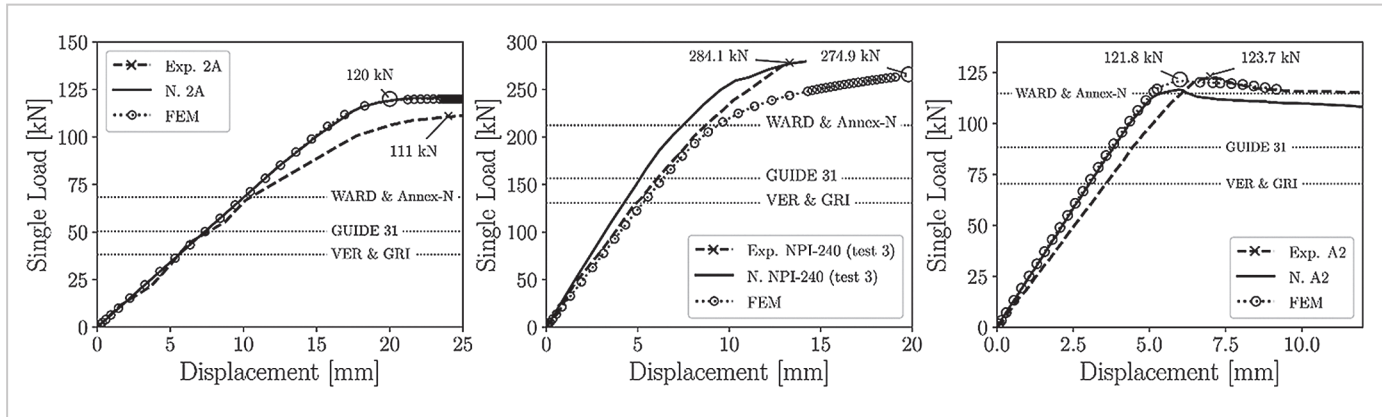


Figure 5 – Single Load versus displacement at the mid-span of cellular steel beams.

In addition, these beams are verified according to the design methods analyzed in herein. Figure 5 shows the failure load (kN) calculated by the

five methods considering the factor of safety as 1.0, which indicates that the formulations of Ward (1990) and Annex-N (1993) have closer results to

those of the experimental tests. It is highlighted that the formulations of these two methods are equal for these cellular beams.

#### 4. Geometric parameter selection and analysis types

In the parametric analysis, the geometrical parameters of cellular beams made from the regular I-section W310x21.0 are varied, to analyze the results of the design methods. The geometric ratio  $p/D_o$  assumes the values: 1.1, 1.2, 1.3, 1.4, 1.5; the ratio  $D_o/d$  assumes the values: 0.9, 1.0, 1.1, 1.2; and the expansion ratio ( $k = d_g/d$ ) has a fixed value of 1.5.

The span variations are determined based on the total height of the cellular beam. These beams are classified according to the  $L/d_g$  ratio:

5 – very short span beam; 10 – short span beam; 15 – long span beam; and 20 – very long span beam. In total, the parametric analysis evaluates 80 cellular beams. The structures are fully laterally braced to prevent failure due to lateral-torsional buckling (LTB). Stiffeners were also employed at the supports to mitigate premature failure.

All beams were evaluated using the design methods outlined in Section 2, considering uniformly distributed loads, and the safety factor as 1.0. Additionally, they were

modeled with FEM analysis, taking an elasto-plastic material with hardening, with an elastic modulus ( $E$ ) of 200 GPa, Poisson’s ratio ( $\nu$ ) of 0.3, yield strength ( $f_y$ ) of 345 MPa, and ultimate stress ( $f_u$ ) of 450 MPa. It is noteworthy that this research focuses on evaluating failure modes considered by the design methods. Thus, it is necessary to consider initial geometric imperfections in nonlinear analyses. Therefore, an amplitude of  $d_g/600$  was adopted for the first elastic instability mode.

#### 5. Parametric Analysis

The aim of the parametric analysis is to assess the performance of the five design methods for cellular beams in comparison to the values obtained through numerical analysis using the FEM in Ansys. Figure 6 shows the four graphs generated corresponding to the specific  $D_o/d$  ratios. Furthermore, the comparison between the methods and the numerical simulation is presented in a normalized format, as follow:  $F_{MTH}/F_{FEM}$ , where  $F_{MTH}$  is the design method load and  $F_{FEM}$  is the load obtained from the finite element simulation, both expressed in kN/m.

In general, the cellular beam results by design method formulation exhibited lower values compared to the reference (FEM results). However,

for beams classified as very short spans ( $L/d_g = 5$ ), the design methods generated higher values than those obtained through FEM. It should be noted that design limit loads for longer beams reached a state of stabilization. This answer occurs because excessive deflection governs the limiting criterion for these beams. Although each design method employs a simplified deflection calculation methodology, this study adopted the vertical displacement limit of  $L/250$ , as recommended for roof beams by the NBR 8800 (ABNT, 2008).

Table 4 contains the analysis of the results showing the Mean Relative Difference ( $\mu$ ), obtained by Equation 2, and the Standard Deviation

of the Mean Relative Difference ( $\sigma$ ), obtained by Equation 3, of the values obtained by the design methods compared to the results in FEM analysis. The WARD method exhibits higher  $\mu$  values for higher  $L/d_g$  ratios, indicating a tendency to overestimate the load capacity. While for shorter beams, lower  $L/d_g$  ratios, WARD brings results closer to those found in FEM analysis. Regarding  $\sigma$ , the GRI method exhibits the greatest variability in relation to  $\mu$ , followed by the VER method. The Annex-N method demonstrated less data dispersion, but it is important to highlight that because this method has a more restricted applicability limit, only 12 beams of each  $L/d_g$  ratio were evaluated.

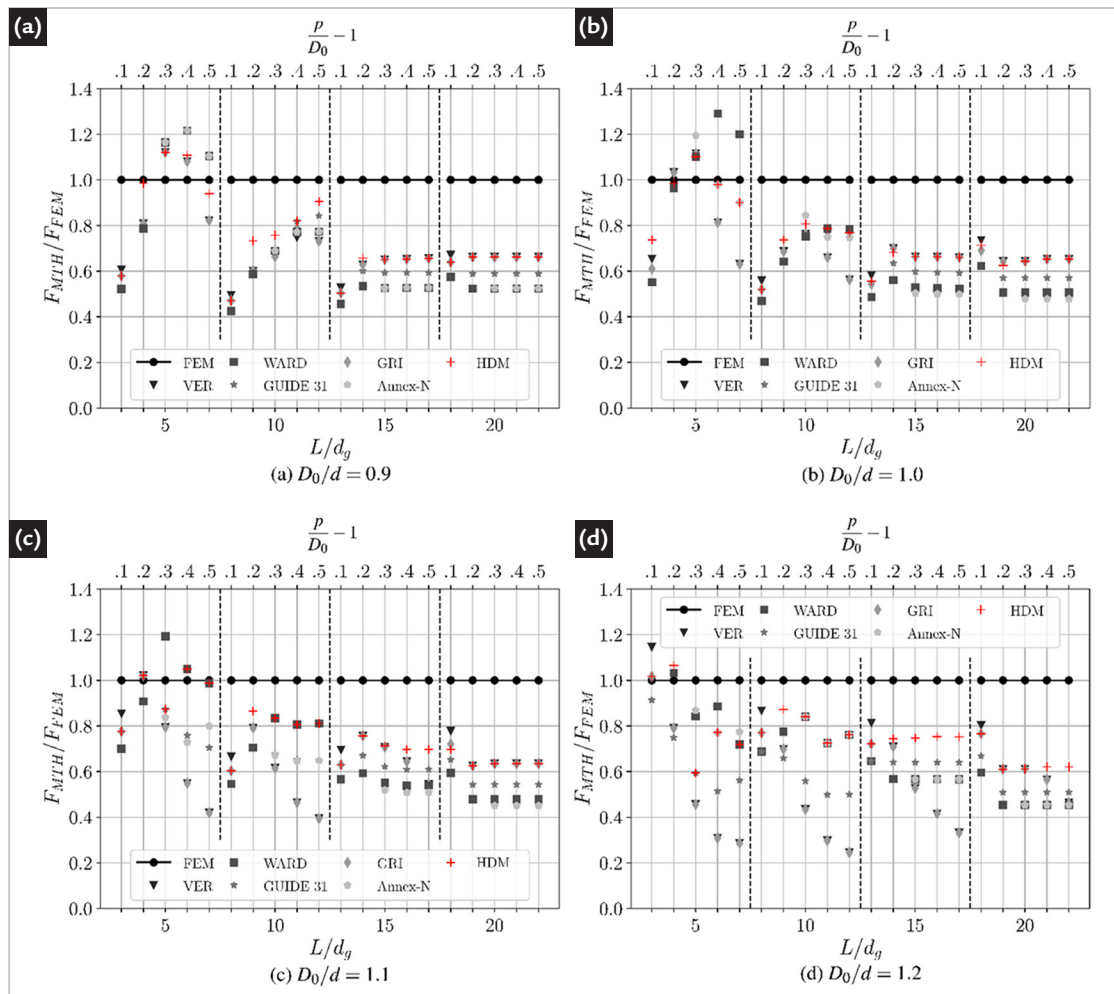


Figure 6 – Scatter plots of numerical results versus the design methods results.

$$\mu = \frac{100}{n} \sum_{i=1}^n \frac{|F_{MTH_i} - F_{FEM_i}|}{F_{FEM_i}} \quad (2)$$

$$\sigma = \sqrt{\frac{1}{n} \sum_{i=1}^n \left( \frac{|F_{MTH_i} - F_{FEM_i}|}{F_{FEM_i}} \cdot 100 - \mu \right)^2} \quad (3)$$

Table 4 - Statistical results of the design methods compared with FEM analysis (%).

$L/d_g$	VER		WARD		GUIDE 31		GRI		Annex-N		HDM	
	$\mu$	$\sigma$	$\mu$	$\sigma$	$\mu$	$\sigma$	$\mu$	$\sigma$	$\mu$	$\sigma$	$\mu$	$\sigma$
5	22.075	12.876	19.765	11.173	23.034	12.720	28.713	18.621	16.828	13.977	13.278	10.255
10	33.122	10.037	29.113	9.189	35.514	9.320	41.172	13.157	26.088	5.238	24.020	7.728
15	32.750	5.231	45.529	2.810	39.869	3.394	38.437	8.271	47.344	2.013	32.212	4.835
20	34.069	3.247	48.814	3.902	43.189	3.354	35.807	3.567	52.323	2.429	34.834	2.656

Figure 7 presents the failure modes detected by the five design methods evaluated with those obtained through FE simulations. In general, the relative mean difference between the limit loads obtained by the methods VER, SCI, Guide 31, GRI, and Annex-N,

and the reference of  $F_{FEM}$  (Table 5) were 30.50%, 35.40%, 35.81%, 36.03%, and 53.47%, respectively. The Annex N (1998) method includes a narrower range of geometric rearrangements, limiting its ability to evaluate all beams. On the other hand, the GRI

method exhibits a higher disparity when compared to VER. Although GRI demonstrates higher accuracy in identifying failure modes, it only detects them when the limit load is lower than the one obtained through the purely VER methodology.

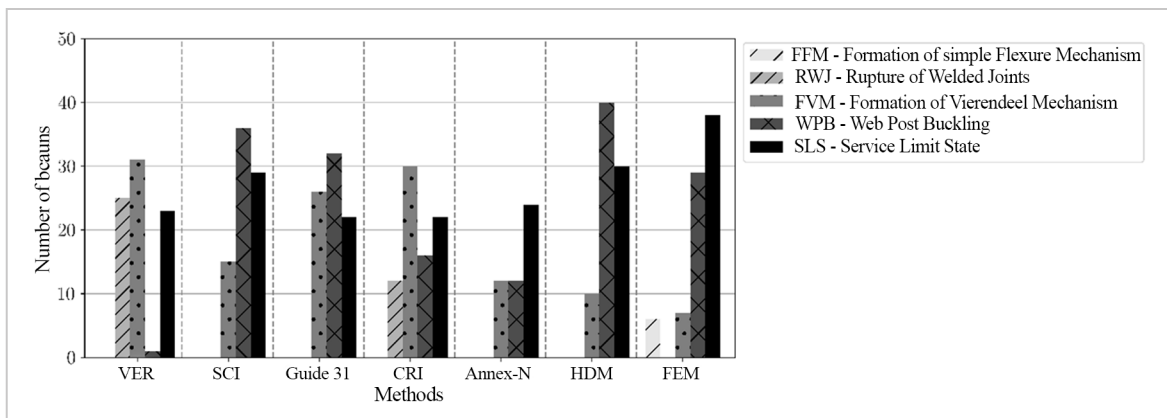


Figure 7 – Failure modes detected by different design methodologies.

By examining the results presented in Figure 7, it is clear that the SCI method more accurately identified the failure modes associated with cellular beams

that failed due to FVM, WPB or SLS in the numerical simulations. The adaptation performed by the GRI method yielded consistent results with FEM analysis when

the beam fails due to FMA. For the Guide 31 method, the beams that failed due to FVM exhibited more conservative limit loads compared to the SCI.

Table 5 - Limit load determined by FEM analysis.

$F_{FEM}$ (kN/m)	$L/d_g$	$p/D_0$	$D_0/d$	$F_{FEM}$ (kN/m)	$L/d_g$	$p/D_0$	$D_0/d$	$F_{FEM}$ (kN/m)	$L/d_g$	$p/D_0$	$D_0/d$	$F_{FEM}$ (kN/m)	$L/d_g$	$p/D_0$	$D_0/d$								
69.4	5	1.1	0.9	59.3	5	1.1	1.0	56.3	5	1.1	1.1	58.7	5	1.1	1.2								
28.5	10			27.9	10			24.2	10			19.5	10										
16.9	15			15.8	15			14.0	15			11.9	15										
9.4	20			8.8	20			8.7	20			8.2	20										
87.4	5	1.2		0.9	84.1	5		1.2	1.0	79.1		5	1.2	1.1		80.9	5	1.2	1.2				
42.7	10				42.2	10				38.3		10				35.1	10						
25.1	15				23.0	15				20.7		15				20.4	15						
10.9	20				10.9	20				10.9		20				10.8	20						
107.5	5	1.3			0.9	99.5		5		1.3		1.0	99.7			5	1.3	1.1		96.2	5	1.3	1.2
54.6	10					48.7		10					49.2			10				39.4	10		
25.5	15					24.4		15					22.3			15				20.5	15		
10.9	20					10.9		20					10.9			20				10.8	20		
118.4	5	1.4	0.9			119.2	5	1.4		1.0	111.2		5		1.4	1.1	104.9			5	1.4	1.2	
58.6	10					55.4	10				51.4		10				45.8			10			
25.4	15					24.6	15				22.8		15				20.5			15			
10.9	20					10.9	20				10.9		20				10.8			20			
130.6	5	1.5		0.9		127.1	5	1.5	1.0		116.1		5	1.5	1.1		119.9		5	1.5	1.2		
58.5	10					55.6	10				51.2		10				43.6		10				
25.5	15					24.7	15				22.8		15				20.5		15				
10.9	20					10.9	20				10.9		20				10.8		20				

### 5.1 Hybrid Design Method for cellular beams

Although the results and the mode of failure detection of the design methods differ from FEM analysis, there is still an association for particular geometries. Thus, a Hybrid Design Method (HDM) is proposed to improve the identification of failure modes and to approximate the limit

loads with the reference of the numerical simulations. The selection of verifications within this hybrid approach is primarily based on the failure mode (Figure 7), followed by the verification that closely corresponds to the limit load (Figure 6). It was verified that the HDM resulted in values

closer to the limit loads found by the FE simulations, having a relative mean difference of approximately 26.08%. Moreover, HDM detection is more accurate when compared to FEM analysis. The proposed Hybrid Design Method is detailed in the next section.



### 5.1.1 Designer ratios parameters required

The limits of applicability are shown in Equation 1, and the slenderness of the

web-post ( $\lambda_{wp}$ ) is verified by Equation 4. Where  $L_M$  is the length between the

mid-height of the web and the point of tangency of the circular opening.

$$\lambda_{wp} = LM \sqrt{12/t_w} \quad \text{with} \quad LM = 0.5 \sqrt{p^2 - D_0^2} \quad (4)$$

### 5.1.2 Overall beam flexural capacity

The overall beam flexural verification is consistent with Ward (1990). In addition, the cellular beam's maximum

bending moment ( $M_u$ ) for Formation Flexural Mechanism (FFM) is determined by Equation 5. This maximum

moment does not exceed the yielding moment ( $M_p$ ).

$$M_u \leq M_p = A_t y f_y \quad (5)$$

### 5.1.3 Beam shear capacity

The verification procedure, recommended by Ward (1990), involves two shear failure modes. The beam's vertical shear capacity ( $P_{vy}$ ) is deter-

mined by summing the shear capacities of the upper and lower Ts. The horizontal shear capacity ( $P_{vh}$ ) is based on the width of the web-post. Equations 6

and 7 present this verification process, where  $V_h$  is the horizontal shear developed in the web-post due to the change in axial forces in the T.

$$V_{sd} \leq P_{vy} = 2 \left( 0.6 f_y 0.9 [(h_t - t_f) t_w] \right) \quad (6)$$

$$V_h \leq P_{vh} = 0.6 f_y (0.9 t_w b_w) \quad (7)$$

### 5.1.4 Web-post flexural and buckling strength

The bending and buckling capacity of the web-post is verified using Ward's (1990) recommendation, later incorporated by AISC Guide

31, according to Equation 8 when  $D_0/d > 1.05$  and  $p/D_0 > 1.25$ , or  $D_0/d < 1.05$  and  $p/D_0 > 1.35$ . Where  $M_{max}$  is the maximum allowable web-

post moment,  $M_e$  is an elastic bending moment and C1, C2, and C3 are calculation constants shown in Equation 9.

$$\frac{M_{max}}{M_e} = \left[ C_1 \left( \frac{p}{D_0} \right) - C_2 \left( \frac{p}{D_0} \right)^2 - C_3 \right] \quad (8)$$

$$\begin{cases} C_1 = 5,097 + 0,1464 \left( \frac{D_0}{t_w} \right) - 0,00174 \left( \frac{D_0}{t_w} \right)^2 \\ C_2 = 1,441 + 0,0625 \left( \frac{D_0}{t_w} \right) - 0,000683 \left( \frac{D_0}{t_w} \right)^2 \\ C_3 = 3,6457 + 0,0853 \left( \frac{D_0}{t_w} \right) - 0,00108 \left( \frac{D_0}{t_w} \right)^2 \end{cases} \quad (9)$$

On the other hand, when the geometric relationships do not follow

the previous applicability ratios, the proposed procedure to avoid WPB is

based on Grilo *et al.* (2018), according to Equation 10.

$$V_{h,p} = \chi \beta f_y \frac{t_w b_p^2}{\sqrt{3b_p^2 + 16y_p^2}} > V_h, \quad \text{with} \quad y_p = \frac{D_0}{2} \left[ 0.445 \left( \frac{p}{D_0} \right)^2 - 2.578 \left( \frac{p}{D_0} \right)^2 + 2.475 \right] \quad (10)$$

Where  $y_p$  is a critical failure distance to  $b_p$  (Figure 1), and  $\chi$  and  $\beta$  are adjustment factors, presented by Grilo *et al.* (2018).

### 5.1.5 Vierendeel bending of upper and lower tees

For the geometry of the cellular beams that follows the ratios  $L/d_g \leq 5$ ,  $p/D_0 > 1.2$ , and  $D_0/d > 1.1$ , or  $L/d_g \leq 10$ ,  $p/D_0 > 1.2$ , and  $D_0/d \leq 1.1$ , it is proposed to use the verification contained in AISC Guide 31 by Fares *et al.* (2016), which

is based on AISC Specifications 360 (2016). Otherwise, the critical section for the T should be determined using the method described by Olander's or Sahmel's approach, as recommended in Ward (1990). Equation 11 should be

used to verify the combined forces in the T to ensure accuracy. In this equation,  $P_o$  and  $M_o$  are the force and the moment on the section.  $P_u'$  is the area of critical section x yield strength,  $M_p'$  is the yielding moment of the critical section.

$$\frac{P_o}{P_u'} + \frac{M_o}{M_p'} < 1.0 \quad (11)$$

### 5.1.6 Serviceability limit state

It is recommended to follow the design method proposed by Veríssimo *et al.* (2013) to verify the displacement at mid-span

( $\Delta_T$ ) of the cellular beam. This verification considers the displacement resulting from bending deflection and shear deformation

$$\Delta_T = \frac{5}{384} \frac{qL^4}{EI_e} + \frac{qL^2}{8GA_e} \quad (12)$$

(Equation 12), which are assessed using the equivalent inertia ( $I_e$ ) and area ( $A_e$ ), presented in Veríssimo *et al.* (2013).

## 6. Conclusions

This paper analyzed five design methods for cellular beams in comparison to Finite Element Method (FEM). Firstly, the FE model was validated using experimental test results from Warren (2001), Erdal & Saka (2013), and Grilo *et al.* (2018). Simultaneously, conservative results were obtained by the design methods for these beams because they are subjected to a concentrated load without stiffeners. Therefore, a nonlinear FEM analysis considering initial geometric imperfections is recommended in these cases.

Then, a parametric analysis of 80 cellular beams was performed, based on simply supported beams with varying geometries, subjected to uniformly distributed loads. The results showed that the Ward (1990)

method best identified the failure modes by FMV and WPB. On the other hand, the adaptation of the Veríssimo *et al.* (2013) method with the WPB check by the Grilo *et al.* (2018) method was more susceptible to detect WPB. However, these methods underestimated the strength of the beams that failed due to FFV. In general, the design methods provided a suitable approximation to the results obtained by finite element analyses for the cases of long and very long beams, with the VER and SCI methods, resulting in a relative mean difference between 30.50% and 35.40%, respectively. Regarding the very short beams, some results were against safety, hence, it's crucial to be cautious when implementing design methods in these cases, and a nonlinear FEM analysis

considering initial geometric imperfections is recommended.

In order to enhance the effectiveness of the analyzed design methods, a Hybrid Design Method (HDM) has been proposed, integrating five distinct design methods. Subsequently, the HDM was employed to verify 80 different cellular beams, resulting in limit load values that were 27.38% to 4.42% closer to the results of FEM when compared to the other five design methods. Despite the superior performance demonstrated by the HDM, it is still recommended to employ nonlinear FEM with initial geometric imperfections for the design process of very short beams. Finally, for the wide use of HDM, it is necessary to expand the parametric analyses to other groups of beams.

## References

- AGUIAR, L. A. *Análise paramétrica sobre procedimentos para dimensionamento de vigas alveolares de aço*. 2023. 180 f. Dissertação (Mestrado em Engenharia Civil) - Universidade Federal do Rio Grande do Sul, 2023.
- AN AMERICAN NATIONAL STANDARD. *AISC 360-16*: specification for structural steel buildings. United States of America, 2016. 676 p.
- ASSOCIAÇÃO BRASILEIRA DE NORMAS TÉCNICAS. *ABNT NBR 8800*: projeto de estruturas de aço e de estruturas mistas de aço e concreto de edifícios. Rio de Janeiro, 2008. 247 p.
- BAKE, S. *Behaviour of cellular beams and cellular composite floors at ambient and elevated temperatures*. 261 f. These (Doctor) - University of Manchester, Manchester, UK, 2010.
- BENINCÁ, M. E. *Simulação numérica de vigas alveolares mistas de aço e concreto*: modelo parametrizado de elementos finitos. 206 f. Dissertação (Mestrado em Engenharia Civil) - Universidade Federal do Rio Grande do Sul, 2018.
- BENINCÁ, M. E.; MORSCH, I. B. Numerical simulation of composite steel-concrete alveolar beams: web-post buckling, Vierendeel and flexural mechanisms. *Latin American Journal of Solids and Structures*, v. 17, n. 5, 2020.
- BRAGA, J. J.; LINHARES, D. A.; CARDOSO, D. C.; SOTELINO, E. D. Failure mode and strength prediction of laterally braced Litzka-type castellated beams. *Journal of Constructional Steel Research*, v. 184, 2021.
- CHUNG, K. F.; LIU, T. C. H.; KO, A. C. H. Investigation on vierendeel mechanism in steel beams with circular web openings. *Journal of Constructional Steel Research*, v. 57, n. 5, p. 467-490, 2001.
- CIMADEVILA, F. J. E.; GUTIERREZ, E. M.; RODRIGUEZ, J. A. V. *Vigas alveoladas*. Madri: Bellisco, 2000. v. 3.
- ERDAL, F.; SAKA, M. P. Ultimate load carrying capacity of optimally designed steel cellular beams. *Journal of Constructional Steel Research*, v. 80, p. 355-368, 2013.
- EUROPEAN COMMITTEE FOR STANDARDIZATION - CEN. ENV 1993-1-1. *Eurocode 3*: design of steel structures - Part 1-1 - General rules and rules for building. Amendment A2: N: Openings in webs (draft). Europe, 1998.
- FARES, S.; COULSON, J. DINEHART, D. *AISC design guide 31*: castellated and cellular beam design, American Institute of Steel Construction, USA, 2016.
- GRILO, L. F. *Formulação para determinação da força cortante resistente de flambagem do montante de alma em vigas celulares de aço*. 199 f. Tese (Doutorado em Engenharia de Estruturas) - Universidade Federal de

- Minas Gerais, 2018.
- GRILO, L. F.; FAKURY, R. H.; VERÍSSIMO, G. S. Design procedure for the web-post buckling of steel cellular beams. *Journal of Constructional Steel Research*, v. 148, p. 525-541, 2018.
- HOSAIN, M. U.; SPEIRS, W. G. Experiments on castellated steel beams. *Welding Journal*. Miami, Fla. v. 52, p. 329-342, 1973.
- KERDAL, D.; NETHERCOT, D. A. Failure modes for castellated beams. *Journal of Constructional Steel Research*, v. 4, n. 4, p. 295-315, 1984.
- LAWSON, R. M. Design for openings in the webs of composite beams. *Steel Construction Institute*, 1988.
- LAWSON, R. M.; HICKS, S. J. Design of composite beams with large web openings: in accordance with Eurocodes and the UK National Annexes. *Steel Construction Institute*, 2011.
- PANEDPOJAMAN, P.; THEPCHATRI, T.; LIMKATANYU, S. Novel design equations for shear strength of local web-post buckling in cellular beams. *Thin-Walled Structures*, v. 76, p. 92-104, 2014.
- SHAMASS, R.; GUARRACINO, F. Numerical and analytical analyses of high-strength steel cellular beams: a discerning approach. *Journal of Constructional Steel Research*, v. 166, 2020.
- SOLTANI, M. R.; BOUCHAÏR, A.; MIMOUNE, M. Nonlinear FE analysis of the ultimate behavior of steel castellated beams. *Journal of Constructional Steel Research*, Elsevier Ltd, v. 70, p. 101-114, 2012.
- SONCK, D. *Global buckling of castellated and cellular steel beams and columns*. 349 f. Thesis (Doctor) - Ghent University, Zwijnaarde, Belgium, 2014.
- SONCK, D.; BELIS, J. Lateral-torsional buckling resistance of cellular beams. *Journal of Constructional Steel Research*, Elsevier Ltd, v. 105, p. 119-128, 2015.
- TSAVDARIDIS, K. D.; D'MELLO, C. Web buckling study of the behaviour and strength of perforated steel beams with different novel web opening shapes. *Journal of Constructional Steel Research*, v. 67, n. 10, p. 1605-1620, 2011.
- VERÍSSIMO, G. S.; VIEIRA, W. B.; SILVEIRA, E. G.; RIBEIRO, J. C. L.; PAES, J. L. R.; BEZERRA, E. M.; CASTRO E SILVA, A. L. R. Estados limites aplicáveis às vigas alveolares de aço. *Revista de Estrutura de Aço*, v. 2, n. 2, p. 126-144, 2013.
- WARD, J. K. *Design of composite and non-composite cellular beams*: publication nº100. Ascot, UK, 1990.
- WARREN, J. *Ultimate load and deflection behavior of cellular beams*. 162 f. Thesis (Master) - University of Natal, Durban, 2001.

---

Received: 13 July 2023 - Accepted: 1 February 2024.